

**Synthesis, thermal and surface activity of cationic single chain metal hybrid surfactants
and their interaction with microbes and protein.**

Gurpreet Kaur^{a}, Preeti Garg^a, Baljinder Kaur^a, Ganga Ram Chaudhary^{*a}, Sandeep Kumar^b,
Neeraj Dilbaghi^b, P. A. Hassan^c, V. K. Aswal^d*

^aDepartment of Chemistry and Centre for Advanced Studies in Chemistry, Panjab University,
Chandigarh 160 014, India.

^bDepartment of Bio and Nano Technology, Guru Jambheshwar University of Science &
Technology, Hisar 125 001, Haryana, India.

^cChemistry Division, Bhabha Atomic Research Centre, Trombay, Mumbai-400085, India.

^dSolid State Physics Division, Bhabha Atomic Research Centre, Trombay, Mumbai-400085,
India

Corresponding authors

Gurpreet Kaur (gurpreet14@pu.ac.in)

Tel: 911722534431

Ganga Ram Chaudhary (grc22@pu.ac.in)

Fax: +91-172-2545074

Characterization of metallosurfactants: Thermo scientific (FLASH 2000) analyzer was used to carry out the elemental analysis (C, H, and N contents). FTIR spectra analyses were made using Perkin Elmer Spectrum 400 (FT-IR/FT-FIR) spectrophotometer with 100 number scans and 4 cm^{-1} spectral resolution using KBr plates. CCl_4 was used as mulling agent. $^1\text{HNMR}$ was performed on Bruker Advance-II spectrometer using D_2O as internal locking agent. The instrument was operating at 400 MHz. Thermogravimetric analysis was performed on SDT Q600 using aluminium crucibles as a function of increasing temperature at a constant heating rate of 10°C under a nitrogen atmosphere.

Characterization of metallomicelles

To estimate the critical micellization concentration (CMC), conductivity and surface tension measurements were carried out. The conductivity measurements were estimated using PICO conductivity meter (LABINDIA) for different temperature ranging from $25\text{--}40^\circ\text{C}$ ($\pm 0.1^\circ\text{C}$). The error limit for conductivity measurement was $\pm 3\%$. The surface tension experiments were performed using a K20 Kruss tensiometer (ring method) at a controlled temperature (298 K). To get the information of structure of metallomicelles small angle neutron scattering (SANS) experiments were performed using the SANS diffractometer at the Dhruva Reactor, Bhabha Atomic Research Centre, Trombay, India. The diffractometer makes use of neutron velocity selector as a monochromator and the measurements were made at a mean wavelength (λ) 5.2 \AA with a wavelength resolution of 15%. The angular distribution of the scattered neutrons was recorded using a one-dimensional position-sensitive detector (PSD), at a fixed sample to detector distance of 1.8 m. The data were collected over a wave vector transfer [$Q = (4\pi\sin\theta)/\lambda$, where 2θ is the scattering angle] range of $0.017\text{--}0.35\text{ \AA}^{-1}$. The samples were prepared in D_2O and held in a quartz sample holder of 0.5 cm thickness. All the measurements were carried out at a temperature of 300K. The measured SANS data were corrected and normalized to a cross-sectional unit, using standard procedures. SANS studies were carried out on metallo-micellar solutions of metallomicelles at different weight fractions.

Experimental details of Biological activity

Hemolytic Studies: Human erythrocytes were collected from a volunteer then as an anticoagulant EDTA was added. Before preparing the RBC suspension, erythrocytes were separated from the heparinized blood. The blood samples were centrifuged for 10 min at 5,000 rpm. The supernatant was discarded, and the erythrocytes were resuspended in isotonic phosphate buffer saline (pH=7.4) followed by centrifugation at >5000 rpm for 5 min. The washing step was repeated three times. Further, an erythrocyte stock dispersion was

resuspended in PBS (appropriate dilution was made) so that the optical density at $\lambda = 575$ nm was approximately 2, after total hemolysis in the assay (control, 100% hemolysis)²⁶. 500 μ L of erythrocyte stock dispersion was taken and the metallosurfactants at the varied amount (pre micellar, micellar and post micellar concentrations) were added. A total volume of 2 mL was adjusted with PBS. The samples were shaken for 5 min to ensure the complete dispersion of mixture and after that, they were left for equilibration at room temperature for 15 min. In the final step, the samples were centrifuged at a constant speed >5000 rpm for 10 min. The supernatant was then extracted and its absorbance was measured at 414 nm.

Anti-microbial activity: Freshly prepared overnight bacterial cultures were grown on nutrient broth at 37°C and Nutrient agar was autoclaved before spreading the microbial stains. 100 μ L of freshly cultured bacterial strains were spread on agar plates and then tested compounds (40 μ L of 0.05 mg/ml and 0.005 mg/ml) were added in the wells on agar plates. The diameters of inhibition zones (measured in nearest of millimetres) was determined after incubation for 24hr at 37°C. The reported data was average value of triplicate measurement. The diameter of the well was excluded from inhibition zone diameter. Solvent i.e. DCM was used as negative control and it did not show any inhibitory activity.

BSA interaction and binding

For UV-vis absorption spectra, the reference blank was phosphate buffer (0.1 M) pH 7.4 solution. For carrying out absorption studies, BSA solution of 1.25 g/l concentration and a stock solution of each MS complex were prepared in phosphate buffer (0.1M) of pH 7.4.

In SDS-PAGE, the polyacrylamide gel plate was prepared using 14% resolving gel and 5% stacking gel. The stock solutions of BSA samples were prepared in phosphate buffer and the concentration of metallosurfactant was varied from pre-micellar to post-micellar concentration range. Circular dichroism (CD) experiments were carried out at controlled temperature (25°C). All the spectra were collected after background correction within the range from 200 to 290 nm using a cuvette of 1 mm path length. A slit width of 1nm and a scan speed of 50 nm min⁻¹ was employed for the measurements. An average of three scans is reported here.

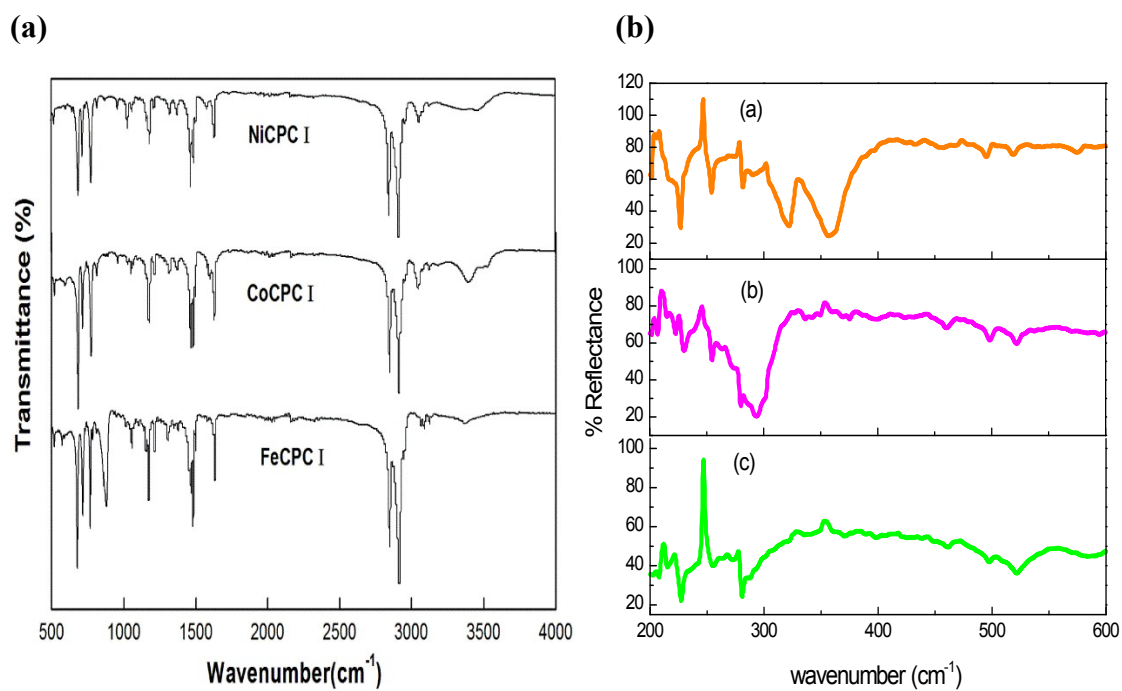


Fig. S1. (a) FTIR and (b) Far-FTIR spectra of metallosurfactants.

Table S1: FTIR and far IR data of CPC and metallosurfactants

Functional group	pure CPC (cm ⁻¹)	NiCPC I (cm ⁻¹)	CoCPC I (cm ⁻¹)	FeCPC I (cm ⁻¹)
Aromatic C-H stretching	3048 3328	3047 3372	3050 3385	3067 3374
-CH ₂ - sym stretching	2912 2848	2912 2848	2915 2849	2915 2849
-CH ₂ -CH ₂ - stretching	1488 1054	1488 1054	1484 1052	1484 1057
C=N and N-C sym stretching	2162 1636 1178	- 1636 1179	- 1634 1177	- 1635 1175
Terminal Cl	325	356	373	357
Bridging M- Cl	-	276	294	282

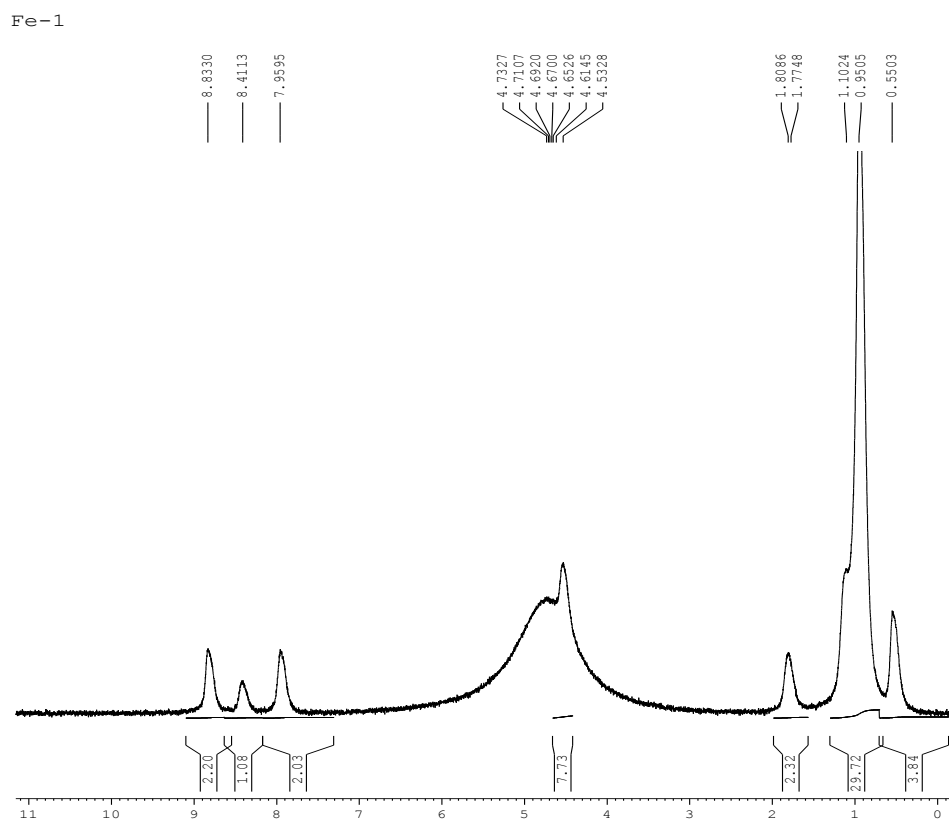
Elemental analyses

For FeCPC I, cal. %C=51.90, %H=7.85, %N=3.02 and obs. %C=52.99, %H=8.14, %N=2.99.

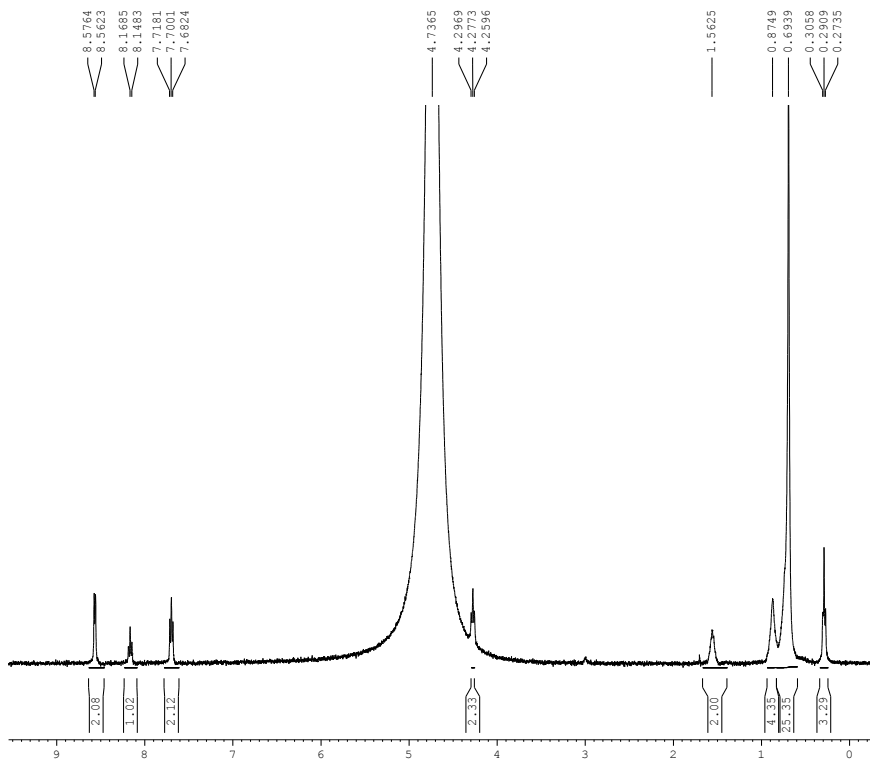
For CoCPC I, cal. %C=56.19, %H=8.60, %N=3.22 and obs. %C=54.63, % H=8.08, %N=2.98.

For NiCPC I, cal. %C=43.90, % H=8.186, %N=2.56 and obs. %C=43.61, % H=7.57, %N=2.42.

¹H-NMR



CO-1



Ni-1

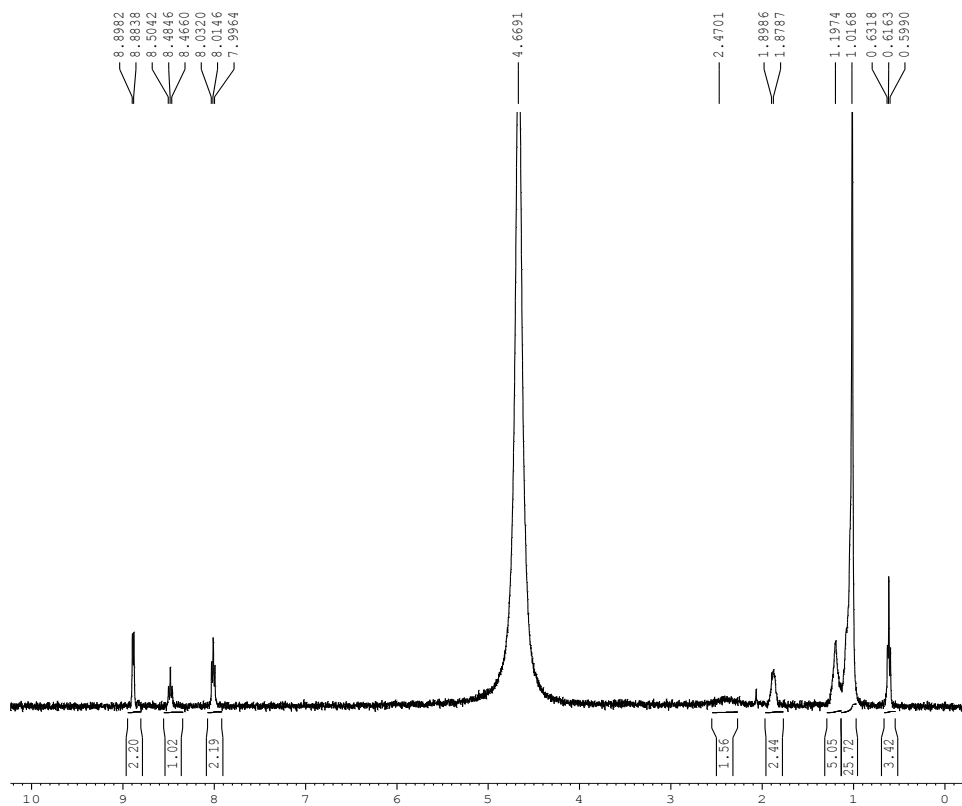


Fig. S2. ¹H-NMR of metallosurfactants

Table S2. ¹H-NMR data of metal-complexes in D₂O.

Complex	v_{Terminal CH₃}	v_{CH₂}	v_{α-CH₂}	v_{β-CH₂}	Aromatic protons
CPC	0.67	1.22	4.62	1.93	8.06 8.50 8.90
FeCPC I	0.55	1.10	4.53	1.80	8.83 8.41 7.95
CoCPC I	0.30	0.87	4.72	1.56	8.50 8.16 7.71
NiCPC I	0.63	1.19	4.66	1.89	8.89 8.50 8.03

TGA

For calculating the kinetic parameters from five methods, the fraction mass loss (α) and corresponding $(1-\alpha)^n$ are calculated from TG curves where n depends upon the reaction model. The details of calculations using different methods are given in following equation S1-S6.

(i) CR method

$$-\log \frac{1-(1-\alpha)^{1-n}}{T^2(1-n)} = \log \frac{AR}{\beta E} \left[1 - \frac{2RT}{E} \right] - \frac{E}{2.303RT} \text{ for } n \neq 1 \quad (\text{S1})$$

$$-\log \frac{-\log(1-\alpha)}{T^2} = \log \frac{AR}{\beta E} \left[1 - \frac{2RT}{E} \right] - \frac{E}{2.303RT} \text{ for } n=1 \quad (\text{S2})$$

A graphical representation between the left-hand side of the above equations against $1/T$ gives a straight line with the slope $(-2.303E/R)$ and the intercept (A) .

(ii) MKN method

$$-\ln \frac{g(\alpha)}{T^{1.9206}} = -\ln \frac{AR}{\beta E} + 3.7678 - 1.9206 \ln E - 0.12040 \frac{E}{RT} \quad (\text{S3})$$

(iii) WYHC method

$$-\ln \frac{g(\alpha)}{T^{1.8946}} = -\ln \frac{AR}{\beta E} + 3.6350 - 1.8946 \ln E - 1.0014 \frac{E}{RT} \quad (\text{S4})$$

(iv) VK method

$$\ln g(\alpha) = \ln \left(\frac{A(0.368/T_m)^{\frac{E_a}{RT_m}}}{\beta \left(\frac{E_a}{RT_m} + 1 \right)} \right) + \left(\frac{E_a}{RT_m} + 1 \right) \ln T \quad (S5)$$

(v) HM method

Parameter $T = T_m + \theta$ is used here. If the order of reaction is 1, T_m is defined as the temperature at which $(1 - \alpha)m = 1/e = 0.368$ and therefore

$$\ln \ln(\alpha) = \frac{E\theta}{RT_m^2} \quad (S6)$$

Here, symbols β , T_m , E , A , Rare heating rate, DTG peak temperature, activation energy (kJmol^{-1}), pre-exponential factor (min^{-1}) and gas constant ($8.314 \text{ Jmol}^{-1}\text{K}^{-1}$), respectively. The excellent correlation coefficients which indicate a good fit of the linear function were obtained for all the methods.

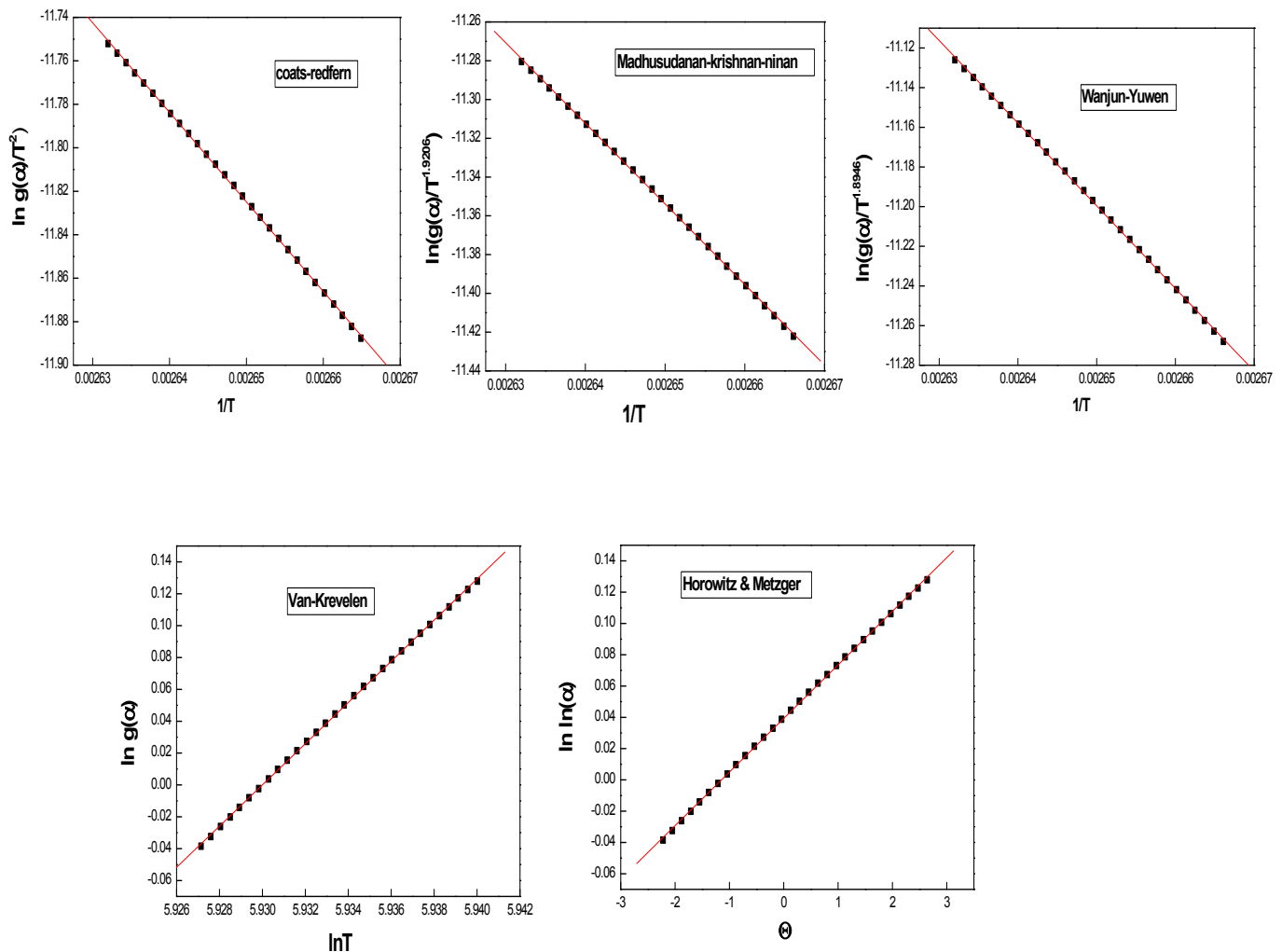


Fig. S3. Linearization curves obtained by different methods for FeCPC I.

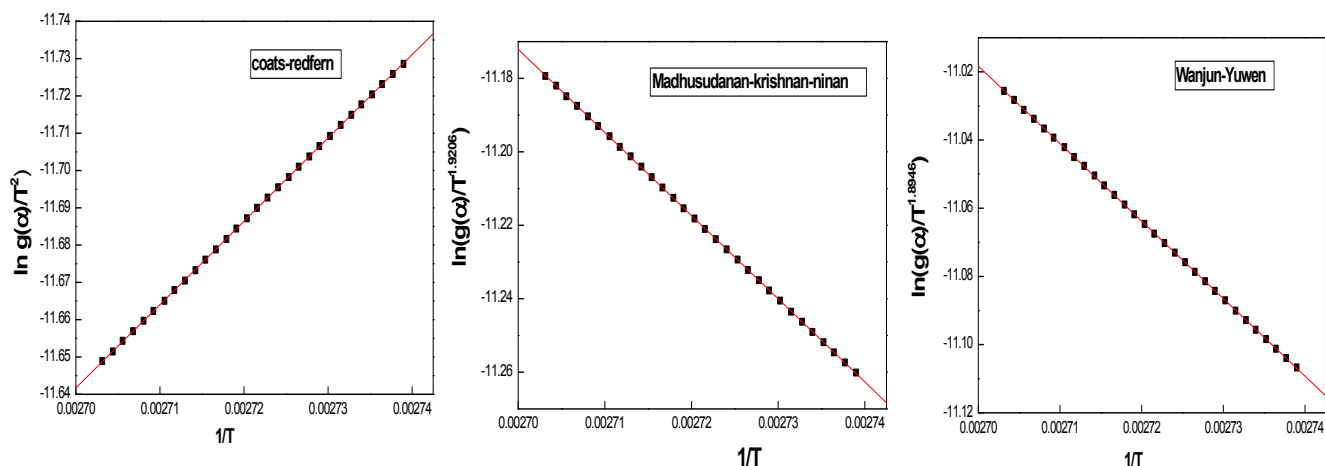
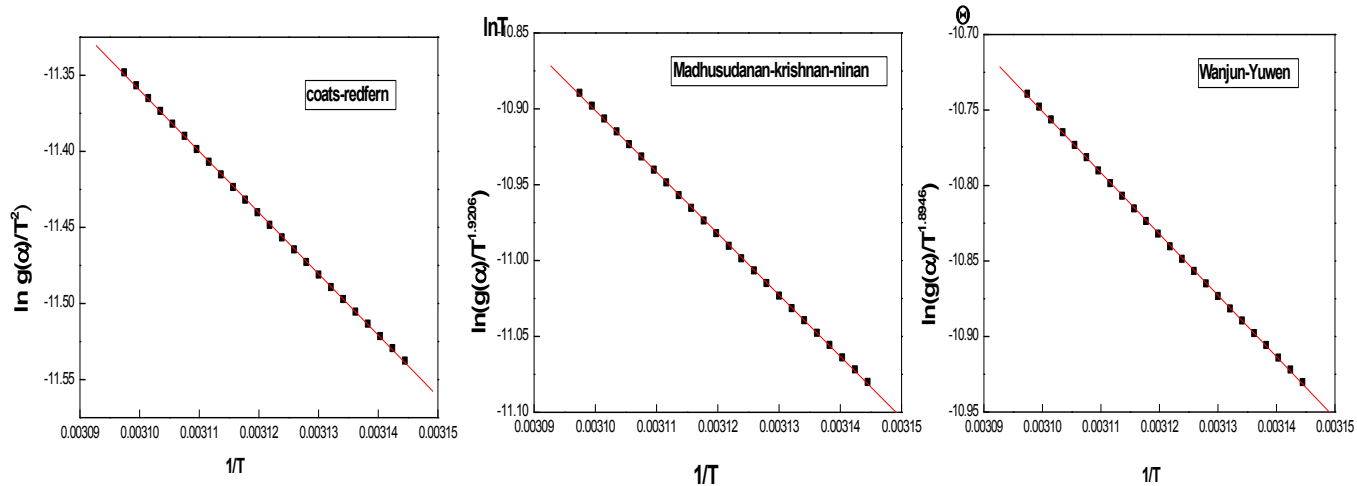
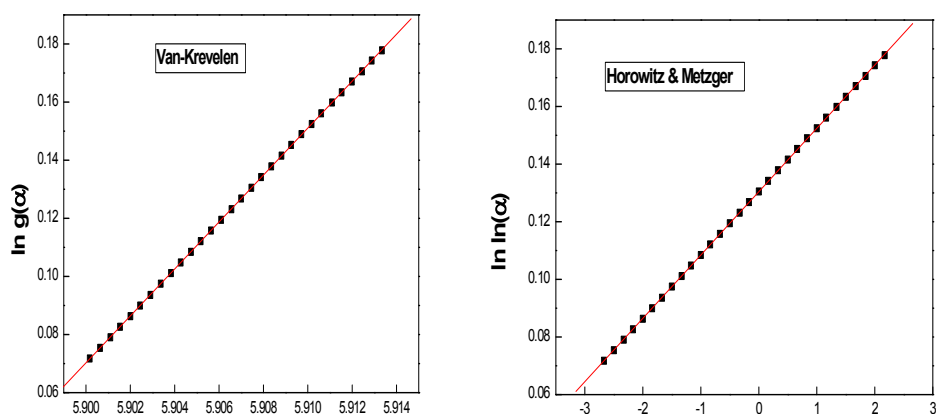


Fig. S4.



Linearization curves

obtained by different methods for CoCPC I.

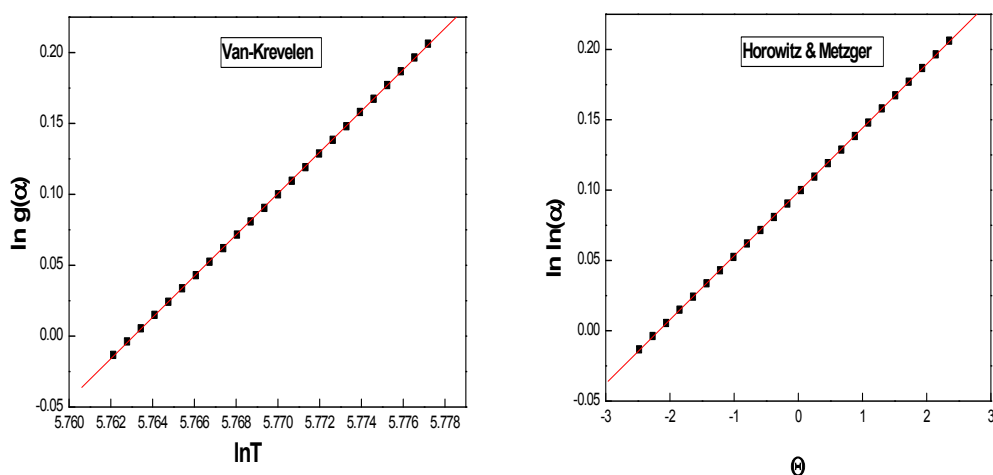
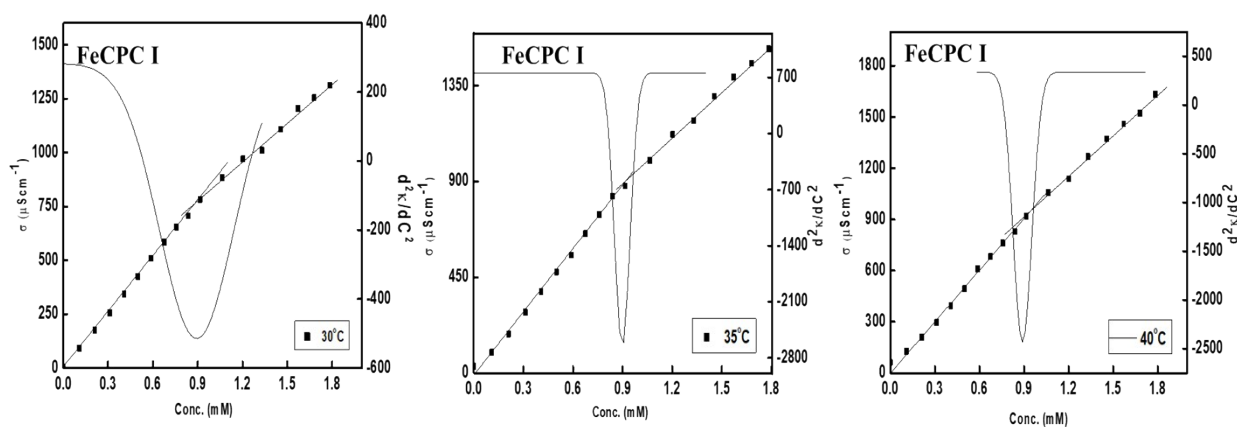


Fig. S5. Linearization curves obtained by different methods for NiCPC I.

Table S3. TGA data and activation energy calculated for metallosurfactants.

Metal complexes	DTG (°C)	Step	Mass loss%		Activation Energy (E/kJmol ⁻¹)				
			Cal.	Obs.	CR	MKN	WHYC	VK	HM
CPC	251.8	I	100	100	40.83	40.87	40.69	45.03	45.20
		II	--	--					
FeCPC I	377.3	I	72.8	71.7	34.24	34.53	34.60	40.55	40.54
		II	15.2	15.1					
CoCPC I	367.7	I	72.3	72.4	18.57	18.79	18.79	24.67	24.71
		II	15.1	15.6					
NiCPC I	320.5	I	58.8	59.9	33.45	33.63	33.69	38.79	38.80
		II	12.2	11.1					



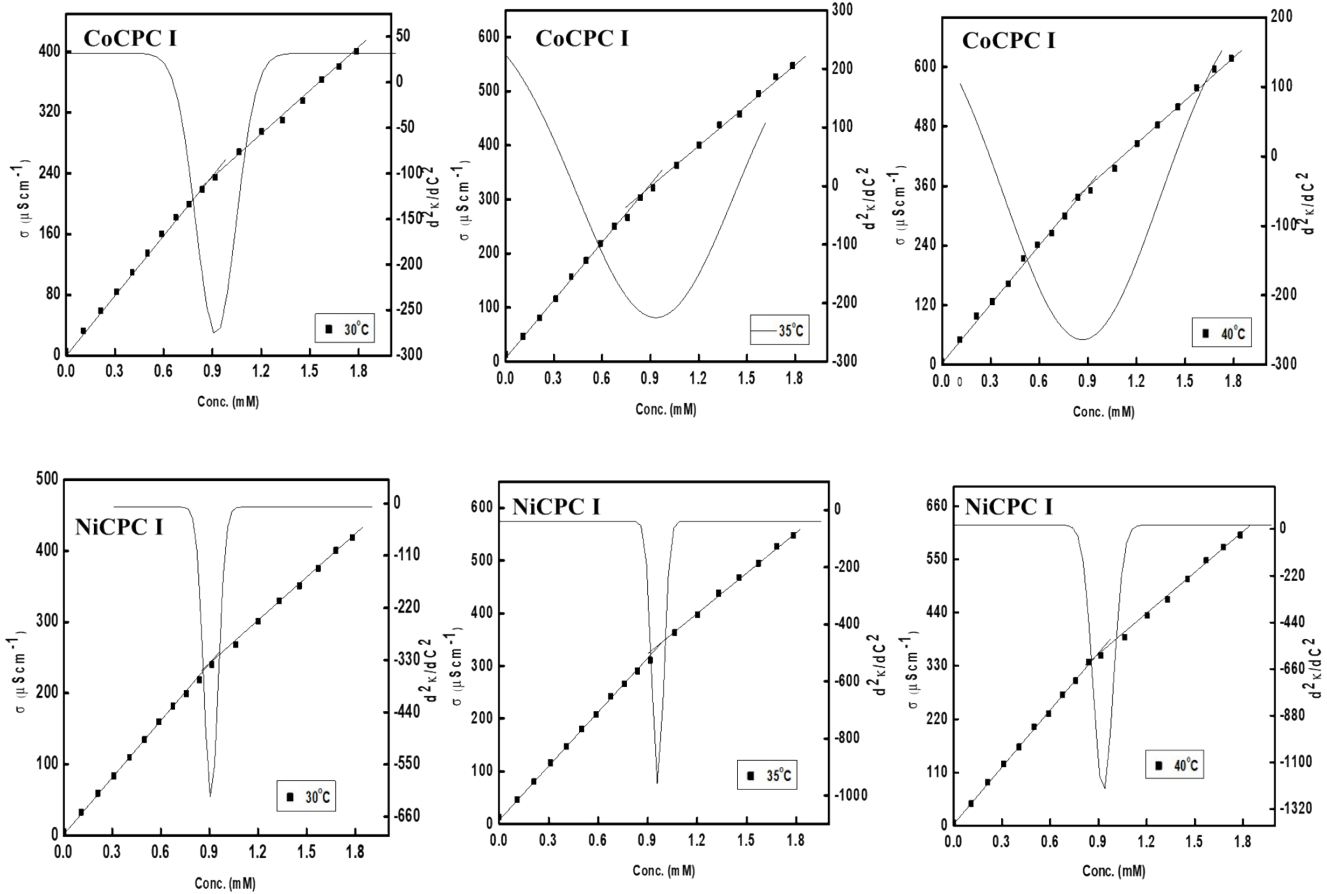


Fig. S6. Conductivity graph of FeCPC I, CoCPC I and NiCPC I metallosurfactants at different temperature.

The micelles formation generally depends upon the thermodynamic parameters i.e. ΔG° , ΔH° and ΔS° are Gibbs free energy, change in enthalpy and change in entropy respectively. These parameters were calculated by using following equations.

$$\Delta G^\circ = (2 - \beta)RT \ln X_{cmc} \quad (S7)$$

$$\Delta H^\circ = -RT^2(2 - \beta)d \ln X_{cmc} / dt \quad (S8)$$

$$\Delta S^\circ = (\Delta H^\circ - \Delta G^\circ) / T \quad (S9)$$

where, R, T, β and X_{cmc} represents gas constant, absolute temperature, the degree of ionization and cmc in terms of mole fraction, respectively.

Surface tension

The maximum surface concentration (Γ_{max}) and the minimum surface area (A_{min}) occupied by single metallosurfactant molecule at interface was calculated by applying the Gibbs adsorption isotherm to the surface tension data.

$$\Gamma_{\max} = -\frac{1}{2.303nRT} \frac{d\gamma}{d \log[C]} \quad (\text{S10})$$

$$A_{\min} = \frac{10^{18}}{N\Gamma_{\max}} \quad (\text{S11})$$

where n is a number of ionic species at the interface (Γ_{CPC} , Γ_{Cl^-} , Γ_{M^+}). ($d\gamma/d \log [C]$), R and T is the surface pressure, universal gas constant and absolute temperature, respectively.

Binding Constant

Stern Volmer equation:

$$\frac{F_0}{F} = 1 + K_{\text{SV}}[Q] \quad (\text{S12})$$

Where F_0 and F is the fluorescence intensity of BSA in absence and presence of metallosurfactant. K_{SV} is the Stern–Volmer quenching constant and $[Q]$ is the concentration of metallosurfactant. This plot gives the straight line which indicates the static quenching of BSA.

The binding constant K_a has been calculated by following equation where n is the number of binding sites.

$$\log \frac{F_0 - F}{F} = \log K_a + n \log[Q] \quad (\text{S13})$$

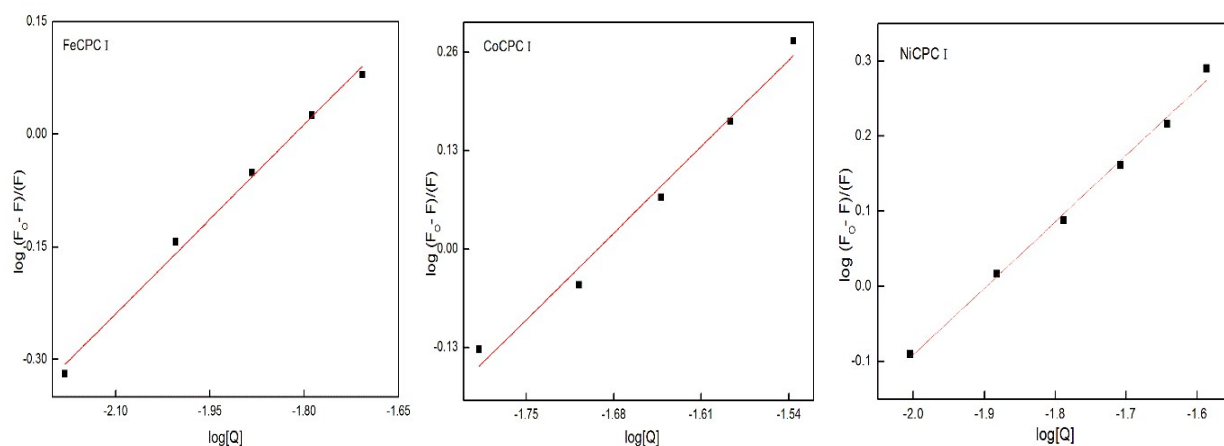


Fig. S7. Plots of binding constant of BSA in presence of different conc. of metallosurfactant (mM) via fluorescence spectroscopy.

Further, to find out the affinity of metallosurfactants (at pre-micellar concentration) for BSA and to compare the effect of metal ion and stoichiometry, Benesi–Hildebrand equation was used.

$$\frac{1}{(A - A_0)} = \frac{\epsilon_G}{\epsilon_{HG} - \epsilon_G} + \frac{\epsilon_G}{\epsilon_{HG} - \epsilon_G} \frac{1}{K_{app}[Q]} \quad (S14)$$

Here, A_0 and A is the absorbance of BSA in the absence and presence of metallosurfactants. K_{app} represents binding constant for a BSA-metallosurfactant system. ϵ_G and ϵ_{HG} is the molar extinction coefficient of the guest in the free form and the bound form.

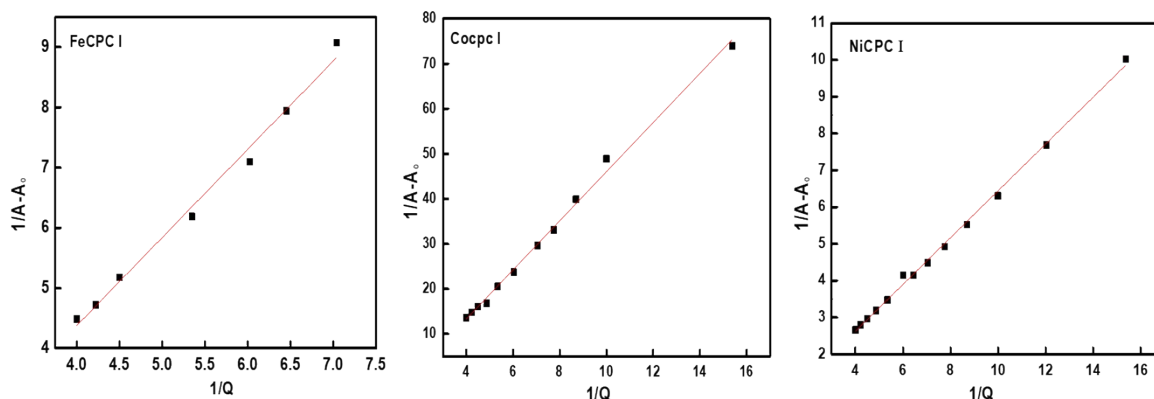


Fig. S8. Plots of binding constant of BSA in presence of metallosurfactant via absorption spectroscopy.

Table S4. Binding constant value of BSA-metallosurfactant complexes.

Complex	K_{app} ($\times 10^3 \text{ Lmol}^{-1}$)	K_{sv} ($\times 10^5 \text{ Lmol}^{-1}$)	K_a ($\times 10^5 \text{ M}^{-1}$)	n
FeCPC I	3.10 ± 0.011	0.66 ± 0.014	0.53 ± 0.008	0.95
CoCPC I	1.55 ± 0.021	0.41 ± 0.011	1.09 ± 0.008	1.20
NiCPC I	0.13 ± 0.005	0.59 ± 0.015	0.47 ± 0.010	0.88

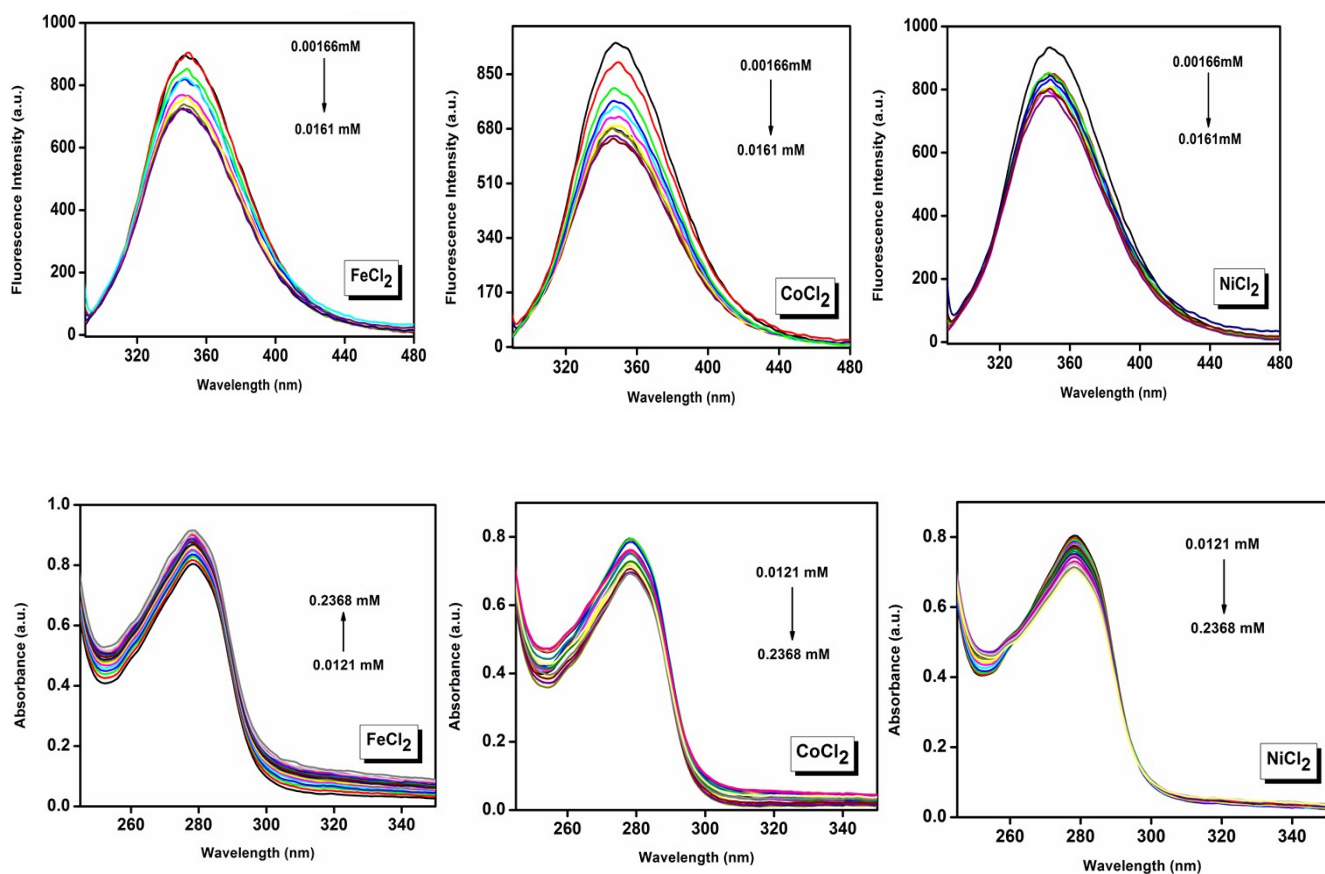


Fig. S9: Fluorescence and UV- vis spectra of BSA in presence of different concentrations of metal salts.

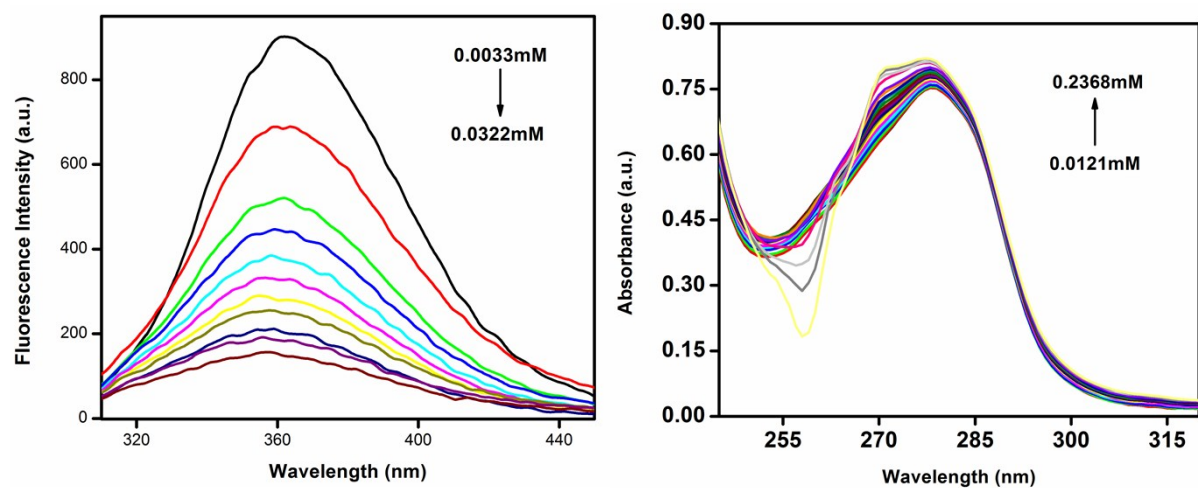


Fig. S10: Fluorescence and UV- vis spectra of BSA in presence of different concentrations of CPC.

The fraction of denaturation protein (F_D) can be calculated as:

$$F_D = \frac{A_{obs} - A_N}{A_D - A_N} \quad (S15)$$

Where A_{obs} is the observed absorbance, A_D and A_N are the absorbance values of denatured and native protein.

Equilibrium constant can be defined in terms of F_D as given by the equation below:

$$K_D = \frac{F_D}{F_N} = \frac{F_D}{1 - F_D} \quad (\text{S16})$$

K_D stands for the equilibrium constant for the denaturation process of protein.

The difference in free energy between the native and denatured conformation (ΔG_D°) of BSA can be calculated as:

$$\Delta G_D^\circ = -RT \ln K_D = -RT \ln \frac{F_D}{1 - F_D} \quad (\text{S17})$$

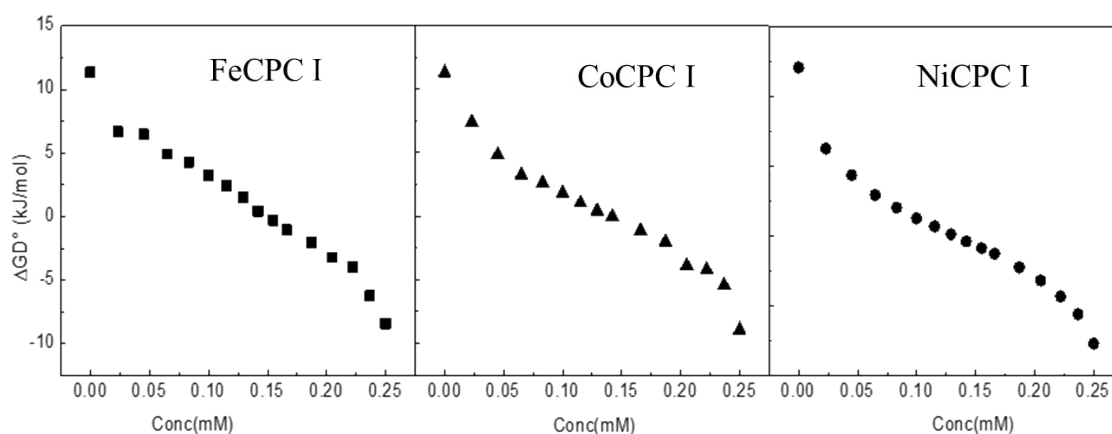


Fig. S11. Plot of ΔG_D° (kJ/mol) vs concentration of metallosurfactant in presence of BSA.

Table S5. Binding constant value of BSA-with metal salts and CPC.

Complex	$K_{sv} (\times 10^5 \text{ Lmol}^{-1})$
CPC	0.95 ± 0.015
FeCl_2	0.19 ± 0.010
CoCl_2	0.22 ± 0.012
NiCl_2	0.076 ± 0.010

Table S6. The α -helix (%) of BSA in presence of various concentrations of different metallosurfactants.

	Concentration	α -helix (%) (at 208 nm)
BSA	0.5 mg/ml	56.41 \pm 0.55
FeCPC I	0.2mM	40.39 \pm 0.82
	0.32mM	39.21 \pm 0.48
	0.8mM	32.05 \pm 0.31
CoCPC I	0.2mM	42.69 \pm 0.86
	0.32mM	42.69 \pm 0.69
	0.8mM	38.41 \pm 0.77
NiCPC I	0.2mM	46.50 \pm 0.60
	0.32mM	45.71 \pm 0.49
	0.8mM	39.23 \pm 0.81

Table S7. Average zone of inhibition against different microbes using prepared metallosurfactants.

	Bacillus polymyza (G+)	Bacillus cereus (G+)	Pseudomonas aeruginosa (G-)	Klebsiella pneumonia (G-)
0.005g/mL (i.e. 10mM) zone of inhibition(diameter in cm)				
CPC	0.4	0.4	0.2	0.2
FeCPC I	0.2	0.2	0.2	0.2
CoCPC I	1	0.9	0.5	0.6
NiCPC I	0.4	0.3	0.4	0.3
0.05g/mL (i.e. 100mM) zone of inhibition(diameter in cm)				
CPC	0.8	0.8	0.6	0.5
FeCPC I	0.5	0.4	0.3	0.3
CoCPC I	1.5	1.0	0.6	0.8
NiCPC I	0.8	0.9	0.7	0.5